Bio-derived and biocompatible poly(lactic acid)/silk sericin nanogels and their incorporation within poly(lactide-*co*-glycolide) electrospun nanofibers

Arisa Kongprayoon[a], Gareth Ross[a,b], Nanteetip Limpeanchob[c], Sararat Mahasaranon[a,b], Winita Punyodom[d,e], Paul D Topham[f], Sukunya Ross[a,b,*]

[a]Department of Chemistry, Faculty of Science, Naresuan University, Phitsanulok 65000, Thailand

[b]Biopolymer Group, Center of Excellence in Biomaterials, Department of Chemistry, Faculty of Science, Naresuan University, Phitsanulok 65000, Thailand

[c]Department of Pharmacy Practice and Center of Excellence for Innovation in Chemistry, Faculty of Pharmaceutical Sciences, Naresuan University, Phitsanulok 65000, Thailand

[d]Center of Excellence in Materials Science and Technology, Chiang Mai University, Chiang Mai, 50200, Thailand

[e]Department of Chemistry, Faculty of Science, Chiang Mai University, Chiang Mai, 50200, Thailand

[f]Aston Institute of Materials Research, Aston University, Birmingham, UK

Phone +6655 963 445, Fax. +6655 963 402, [*]e-mail: sukunyaj@nu.ac.th

Abstract

Bio-derived and biocompatible nanogels based on poly(lactic acid) (PLA) and silk sericin (SS) have been synthesized for the first time. Low molecular weight PLA and SS were first modified using allyl glycidyl ether to create a PLA macromonomer and an SS multifunctional crosslinker (PLAM and SSC, respectively), as confirmed by NMR and FTIR spectroscopies. Nanogels were synthesized from PLAM/SSC and *N*′*N*-methylene bisacrylamide (*N*′,*N*-mBAAm) as an additional bifunctional crosslinker via classical free-radical polymerization at systematically varied levels of additional crosslinking (0, 0.5, 1.0, 1.5 and 2.0 w/w% *N*′,*N*-mBAAm). Higher crosslink densities led to smaller nanogel particles with reduced accumulative drug release. Crosslinked PLAM/SSC nanogels at 0.5% *N*′,*N*-mBAAm with 400-500 nm diameter particles were shown to be non-toxic to the normal

human skin fibroblast cell line (NHSF) and selected for incorporation within poly(lactide-*co*-glycolide) (PLGA) electrospun nanofibers. These embedded nanogel-PLGA nanofibers were non-toxic to the NHSF cell line and exhibited higher cell proliferation than pure PLGA nanofibers, due to their higher hydrophilicity induced by the PLAM/SSC nanogels. This work shows that our new crosslinked-PLAM/SSC nanogels have potential for use not only in the field of drug delivery but also for tissue regeneration by embedding them within nanofibers to create hybrid scaffolds.

1. Introduction

Nanogels are three-dimensional (3D) crosslinked polymeric particles with nanoscale dimensions that are an attractive type of material for use in biomedical applications such as tissue engineering, biomedical implants and drug delivery systems (1,2). This is due to their properties, such as a large surface area for multivalent bioconjugation, interior network for the incorporation of biomolecules, high water content and biocompatibility (3–5). A common use of nanogels is as carriers for antibiotics in the treatment of bacterial infection, which is still a major cause of hospitalization and mortality (6). Research has shown that the use of antibiotics in their free form can cause treatment failure due to low bioavailability, poor penetration to bacterial infection sites, side effects, and antibiotic resistant properties of bacteria (6). Therefore, encapsulation of antibiotics in nanogels or polymeric particles has been utilised to increase efficiency of release at the infection site as well as reducing the dosage and dosing frequency. For this purpose different polymeric micro-to-nanoparticles or gels, sourced from both synthetic and natural polymers, such as poly(*N*-isopropylacrylamide) and poly(acrylic acid) (7), poly(D,L-lactide-*co*-glycolide) (8,9), polycaprolactone (10) and chitosan (11), have been developed to meet different clinical needs.

Poly(L-lactic acid) (PLLA) is a synthetic biodegradable polymer manufactured from renewable resources (i.e. corn, starch, potatoes) and widely used in many applications, such as drug delivery devices, tissue-supporting scaffolds, and film packaging (12,13). It is the L-stereo-regularity of poly(lactic acid) or polylactide (PLA), which occasionally is terminated with carboxylic acid end-chain. Silk sericin (SS) is a glue-like protein that covers the double strands of fibroin of silk cocoons (wild silk and Bombyx mori). SS is comprised of 18 types of amino acids with high essential amino acids of serine, glycine, aspartic acid, glutamic acid, threonine and tyrosine, respectively (14–16). These protein structures consist of hydroxyl, carboxyl and amino functional groups, which make sericin soluble in polar solvents like

water (17,18). Importantly, these strong polar side groups allow for chemical modification with other materials and expand the suitable applications of silk sericin.

Tissue engineering scaffolds are an important family of materials due to the difficulty and complexity of the classical treatments by an autograft or allograft. They are essentially used as a template for the growth of cells to regenerate new tissue without surgical operation (19,20). Scaffolds for skin regeneration are mainly in the form of hydrogel porous structure (14,21,22) and nanofibers (23–26). Nanofibers produced by electrospinning are good candidates for scaffolds, due to their high specific surface area and highly porous structure. This helps to mimic the microscale morphology of the native extracellular matrix (ECM) and allows for enhanced cell migration and proliferation to accelerate wound healing (27). Recently, nanofibers have not only targeted cell migration and proliferation but also have been incorporated with active components for enhanced treatments such as drug delivery (28,29).

Due to the advantages of electrospun nanofibers for skin regeneration and polymeric nanogels for drug delivery, in this work, we have synthesized new polymeric nanogels from fully biodegradable materials [poly(L-lactic acid) (PLLA) and silk sericin (SS)]. These nanogels are then targeted for versatile use as a carrier for drugs, bioactive agents, growth factors or other components. In addition, these nanogels have been embedded within a poly(lactide-*co*-glycolide) (PLGA) electrospun nanofibrous mesh for potential use as tissue engineering scaffolds with dual functionality; drug delivery and tissue regeneration.

Therefore, this present work, started with the synthesis of new polymerizable PLLA (referred to as PLA macromonomer, PLAM) and SS (as SS multifunctional crosslinker, SSC) from low molecular weight PLA and SS, respectively (overview presented in Fig. 1). The chemical structures of PLAM and SSC were analyzed by nuclear magnetic resonance spectroscopy (NMR) and Fourier-transform infrared spectroscopy (FT-IR). Then, novel nanogels of PLAM/SSC were synthesized via classical free radical polymerization in the presence of a crosslinker (*N'N*-mBAAm). The effect of crosslinker concentration on the diameter size and drug release profiles of the nanogels was studied in detail along with their concomitant morphology (by transmittance electron microscopy (TEM)) and cytotoxicity. Furthermore, crosslinked-PLAM/SSC nanogels were embedded within PLGA electrospun nanofibrous scaffolds and this hybrid system characterized by morphology, enzymatic accumulative degradation, hydrophilicity and cytotoxicity.

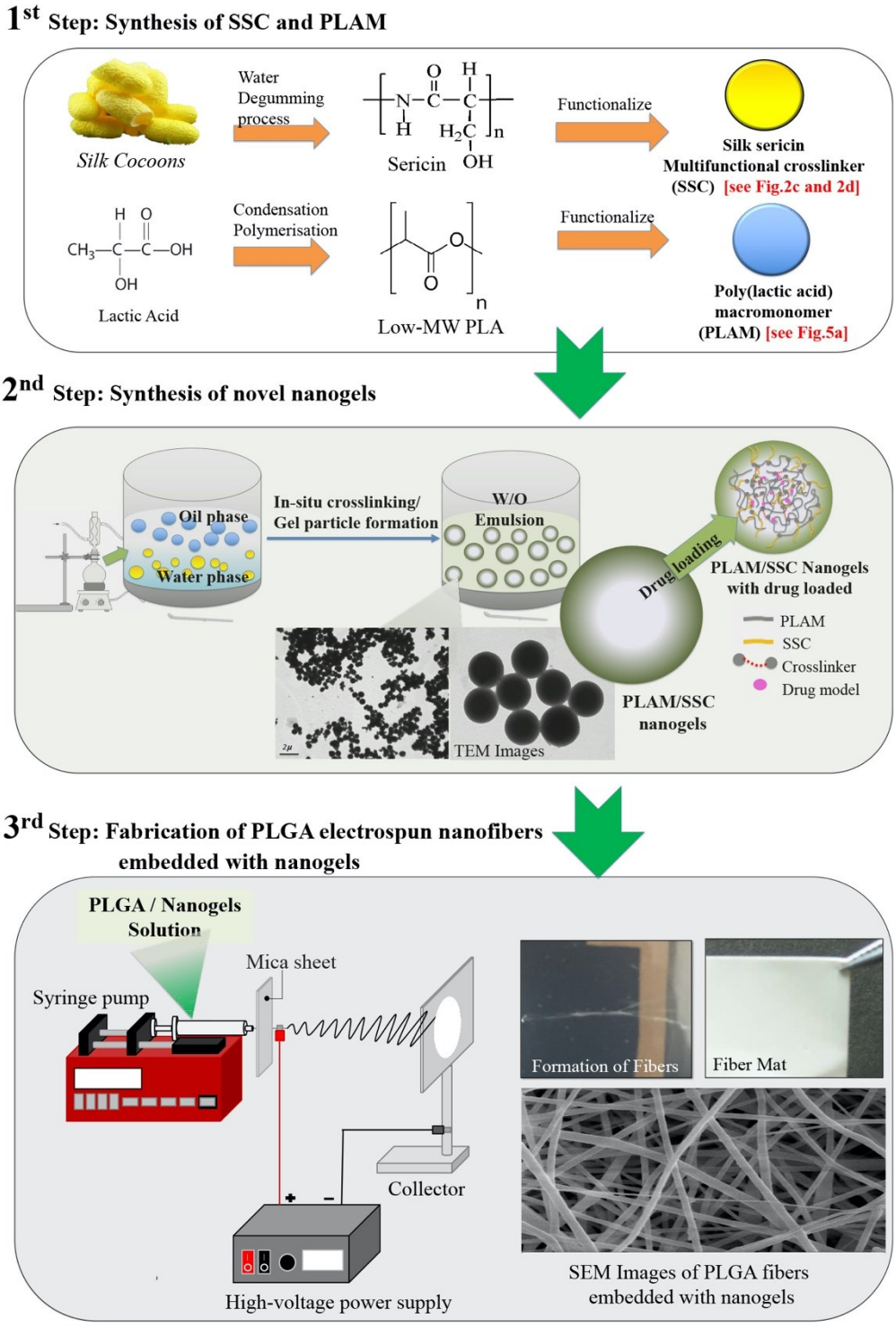

Figure 1. Overview of the synthetic approach adopted in this work.

2. Materials and method

2.1 Materials

Poly(lactic acid) (PLA) with an average weight molecular weight of 2,250 g/mol was used as received from the condensation polymerization of lactic acid. Silk cocoons (Bombyx mori) were provided from Tak province in the lower northern region of Thailand. Allyl glycidyl ether (AGE), zinc (Zn), *N*′,*N*-methylene bisacryamide (*N*′,*N*-mBAAm), *N*-methyl-2-pyrrolidone (NMP), tetramethylethylene diamine (TEMED), dimethyl sulfoxide (DMSO), rhodamine B (model drug) were supplied by Sigma-Aldrich (Singapore). Potassium hydroxide (KOH) and ammonium persulfate (APS) were purchased from Univar chemical. Poly(lactide-*co*-glycolide) (PLGA), at LA:GA ratio of 75:25 with an average molecular weight of 108,000 g/mol, was supplied by bioplastic production laboratory for medical applications, Chiang Mai University. Normal human skin fibroblast cell line (NHSF) was obtained from Japanese collection of research bioresources cell bank (JCRB Cell Bank). XTT (2,3,-bis(2methoxy-4-nitro-5-sulfophenyl)-5-[(phenylamino)carbonyl]-2H-tetra-zolium) was supplied by Thermo Fisher Scientific (Waltham, MA, USA).

2.2 Synthesis of SS multifunctional crosslinker (SSC) and PLA macromonomer (PLAM)

Silk sericin multifunctional crosslinker (SSC)

The first step was the preparation of silk sericin powders by a hot water degumming process following the method used in our previous work (14,21). Briefly, silk cocoons were cut into small pieces with 20 g added to 500 mL of DI water, this was then heated to 100 °C for 4 hrs. After that the SS solution was dried in an oven at 60 °C for 12 hrs to obtain silk sericin powder (SS). To convert SS to SSC the chain-end or pendant carboxylic groups were modified by allyl glycidyl ether (AGE) (see Fig.2b). Initially, 5 wt% of SS was dissolved in 20 mL of DI water and then mixed with 5 wt% AGE and Zn powder (1 wt% of total amount of the reactants) in a close system. The reaction was carried at 70 ºC, under a nitrogen atmosphere with constant stirring for 12 hrs. After that, the reacted solution was added dropwise into cold DI water to remove any unreacted species, this process was repeated three times. The precipitant sample was termed “silk sericin multifunctional crosslinker (SSC)” which was collected and dried at 60 °C for 48 hrs before storing in desiccator to avoid any exposure to moisture.

Poly(lactic acid) macromonomer (PLAM)

A low molecular weight of PLA was selected and the chain-end groups were modified with AGE following a similar procedure to SSC but with slight alterations in the method (see Fig.5a). 5 wt% of low molecular weight PLA was dissolved in 150 mL of dimethyl sulfoxide and then mixed with 5 wt% AGE and 0.5 wt% Zn powder in a close system. The reaction mixture was heated at 70 °C under a nitrogen atmosphere and stirred for 12 hrs. After that, the sample was precipitated with cold DI water three times to remove all residual solvent before drying the sample at 60 °C for 48 hrs. Finally, the dried sample termed "poly(lactic acid) macromonomer (PLAM)" was stored in a desiccator before use.

2.3 Synthesis of PLAM/SSC nanogels

Novel nanogel particles of PLAM/SSC were synthesized via conventional free radical polymerization in the presence of a crosslinker (*N*′,*N*-methylene-bisacrylamide) in an W/O emulsion system. 2 wt% PLAM and 2 wt% SSC were dissolved separately in *N*-methyl-2-pyrrolidone (NMP, the oil phase) and DI water (the water phase), respectively. They were allowed to dissolve for 2 hrs at 70 °C before being mixed together for 30 mins. Then *N*′,*N*-methylene bisacrylamide (*N*′,*N*-mBAAm) was added as the crosslinker, at different concentrations of 0.5, 1.0, 1.5 and 2 %w/w (The reaction was also carried out without crosslinker 0 %w/w). The mixture was then cooled down to 30 °C before adding tetramethylethylene diamine (TEMED) and finally, ammonium persulfate (APS) to start the reaction with stirring for 30 mins. After finishing the reaction, the nanogels were purified by precipitation in cold DI water to remove any residual non-polymerized materials and dried at 60 °C for 48 hrs before storing in a desiccator.

2.4 Fabrication of PLGA electrospun nanofibers embedded with nanogels

The crosslinked-PLAM/SSC nanogels were incorporated into a PLGA solution that was then used to fabricate electrospun nanofibers by a colloid-electrospinning technique. 10 wt% PLGA was dissolved and stirred in 4:1 – chloroform : dimethylformamide (DMF) solution for 24 hrs before the addition of 0.1 wt% crosslinked PLAM/SSC nanogels. The nanogels were suspended in PLGA solution by the incorporation of a surfactant (Pluronic® F-127). The colloid solution was ejected from a 10 mL plastic syringe via a metallic needle (0.7 mm inner diameter) at the distance of 15 cm from the collector, a flow rate of 0.3 ml/hrs and voltage of 25 kV was used. Finally, the electrospun PLGA nanofibers with embedded

nanogels were collected as a mat on the collector. Samples were kept in desiccator to protect from moisture before further characterization.

2.5 Characterizations

Functional groups by FT-IR

Fourier Transform Infrared Spectrometer (FT-IR) from Perkin Elmer (model Spectrum GX) was used to characterize the functional groups of PLAM, SSC and PLAM/SSC nanogels with and without crosslinker. All samples were dried before testing and used the attenuated total reflection (ATR) mode of FT-IR.

Chemical structures by NMR

Nuclear magnetic resonance (NMR) (model Bruker Advance 400) was used to study the chemical structures of PLAM and SSC to confirm that the vinyl groups were successfully added. PLAM and SSC were dissolved in deuterated dimethyl sulfoxide (DMSO-d6) before testing proton (^{1}H) and carbon (^{13}C) NMR.

Morphology by SEM and TEM

Transmission electron microscope (TEM, TECNAI12 PHILIPS model) was used as a tool to observe the size and shape of the nanogels. Briefly, nanogels were suspended in phosphate buffer saline (PBS). Then a drop of sample was placed on copper grids, followed by drying at room temperature before being loaded to the transmission electron microscope. The PLGA electrospun nanofibers embedded with nanogels were also observed for their morphology by TEM. The surface of the electrospun fibers were observed by scanning electron microscope (SEM), 1455VP Leo model, using secondary electron beam with high voltage. Samples were cut and tapped on sample stub before being coated by gold particles.

Contact angle measurement (CA)

Contact angle (Data physics model OCA20) was used to study the hydrophilicity of electrospun nanofibers at room temperature. Water was injected from a syringe onto the surface of the nanofiber mats (1 μL dosing volume). Images of the water droplets were recorded with a video camera and the contact angles of samples determined using the built in OCA software.

2.6 *In vitro* drug release behavior of nanogels

The nanogel particles synthesized with different concentrations of crosslinker were immersed in a constant concentration of Rhodamine B solution (a dye used as model drug). The solution with nanogel particles was constantly stirred overnight to promote saturated-nanogel particles with model drug. Then, these saturated-nanogel particles were separated from the solution by centrifuging before being added 0.5 mL of phosphate-buffered saline (PBS, pH 7.4) and placed in incubator at 37 °C. Aliquots of solution were taken out at appropriate time intervals, while fresh PBS was re-added to maintain the same volume at 0.5 mL. The time intervals were 1, 2, 3, 4, 5, 7, 9, 11, 24, 26, 28, 30, 32 and 48 hours. The concentration of model drug at each time interval was analyzed by Microplate reader (model UV-Vis Biotek synergy H1 Hybrid Reader spectrophotometer) at 544 nm. The cumulative drug release (mg/mL) was calculated by comparing the measured optical density to that of standards of Rhodamine B.

2.7 Enzymatic degradation of electrospun nanofibers embedded nanogels

The electrospun nanofibers embedded nanogel samples were cut into sizes of 1 cm^2 and weighed for the initial weight (W_i). After that, the samples were immersed in 2 mL of 0.004 % trypsin in PBS solution and stored in an incubator at 37 °C. The solution was refreshed every week and the samples were weighed every week, to record the weight after degradation (W_d). The % weight loss was calculated by the following Eq.1:

$$\%Weight\ loss = \frac{W_i - W_d}{W_i} \times 100 \qquad \text{Eq.1}$$

2.8 *In vitro cell* cytotoxicity

The cytotoxicity of nanogels was observed using an XTT assay (indirect method), according to ISO 10993-5 (ISO 10993-5:2009(en) biological evaluation of medical devices - part 5: tests for in vitro cytotoxicity. Human skin fibroblast cells line (NHSF) was seeded in 96-well plates at a density of 10,000 cell/well and allowed to adhere overnight. Nanogels were incubated in DMEM (Dulbecco's Modified Eagle Medium) at 37 °C for 24 h. Then, this nanogels-extracted DMEM (200 µL) was added into wells containing cells and incubated for 24 h before removal. The 200 µL of medium with XTT solution was added into each well and incubated for 4 h before the cell viability test. The cell viability was determined by microplate reader absorbance at 490 nm. The OD value of all samples were compared with a control, the percentage of cell viability was calculated following Eq.2.

$$\text{Cell viability (\%)} = \left|\frac{OD_s}{OD_c}\right| \times 100 \qquad \text{Eq.2}$$

Where ODs is the absorbance of impregnated medium of samples and ODc is the absorbance of a control (untreated cells or cells incubated with culture medium without samples).

2.9 In vitro cell proliferation: XTT

XTT assay was used to study the viability of cells seeded on the samples after 1, 3 and 5 days in culture. The NHSF cell lines were first cultured in a flask with DMEM medium supplemented with 10% v/v fetal bovine serum (FBS), 1%v/v penicillin/streptomycin and 0.1%v/v amphotericin B incubated at 37 °C under 5% CO_2 humidified atmosphere. The culture medium was refreshed every 3 days. The samples were sterilized by ozone and washed with PBS solution before immersing in DMEM containing 10% v/v FBS for 1 h and then left for a further 1 h in an incubator at 37 °C. Afterwards, the NHSF cells (7 x 10^4 cells/well) were seeded on samples for 1, 3 days and 5 days of culture. Cultured samples were transferred and placed into a new 24-well plate with 200 µL of new serum-free medium to which 50 µL of XTT solution was added and left for 4 h in an incubator. Absorbance at 490 nm was measured with a microplate reader.

3. Results and Discussion

Nanogels based on bio-derived and biocompatible poly(lactic acid) (PLA) and silk sericin (SS) have been synthesized for the first time. In this report, we demonstrate the successful chemical modification of both PLA and SS to create a PLA macromonomer (PLAM) and SS multifunctional crosslinker (SSC), respectively. The effect of additional *N*′,*N*-mBAAm crosslinker on the formation of the nanogels is elucidated together with their *in-vitro* drug release profile and cytotoxicity. Finally, we demonstrate the versatility and applicability of the nanogels through incorporation into electrospun PLGA nanofibrous fabrics as hybrid scaffolds for potential use in tissue regeneration.

3.1 SS multifunctional crosslinker (SSC) and PLA macromonomer (PLAM)

SS and PLA were modified by the addition of vinyl groups from allyl glycidyl ether (AGE) onto their chain-ends or side groups, converting them to SSC and PLAM, respectively. ^{1}H and ^{13}C NMR spectroscopies were used to confirm the successful

modification of the chain-ends or side groups of SS and PLA to create the corresponding crosslinker and macromonomer.

Silk sericin multifunctional crosslinker (SSC)

Silk sericin is a protein comprising varying amounts of 18 different amino acids, with the six most common being serine, aspartic acid, glycine, threonine, alanine and glutamic acid (Fig.2a) (14,30–33). This provides tremendous versatility, allowing silk sericin to be modified with a wide range of chemical functionality, such as vinyl groups to convert the protein into a macromonomer or crosslinker, capable of further polymerization. To the best of our knowledge, the synthesis of silk sericin multifunctional crosslinker (SSC) has not been reported previously. The schematic of SS functionalization is shown in Fig.2b,c and d. SS is modified through the reaction of epoxide-functionalized AGE in the presence of zinc, where the reactions can take place at the C- and N-termini of the protein backbone and at the pendant carboxylic acid groups present on the aspartic and glutamic acid units within the protein. The reaction of AGE with the various carboxylic acid groups (terminus and pendant) and amine group (terminus) equips SS with vinyl groups to create a multifunctional SSC capable of polymerization and crosslinking.

a

Silk Sericin Composition
(Showing the 6 most abundant amino acids)

Amino Acid	%
Serine	31.44
Aspartic Acid	17.70
Glycine	14.57
Threonine	8.46
Alanine	4.93
Glutamic Acid	4.79

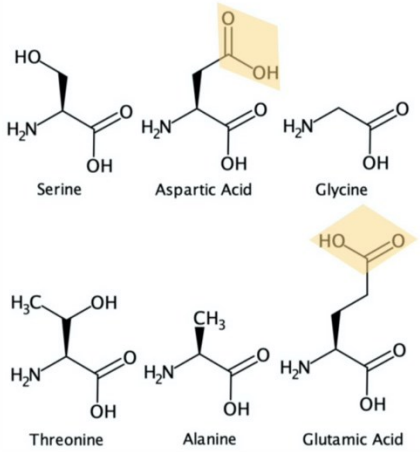

b

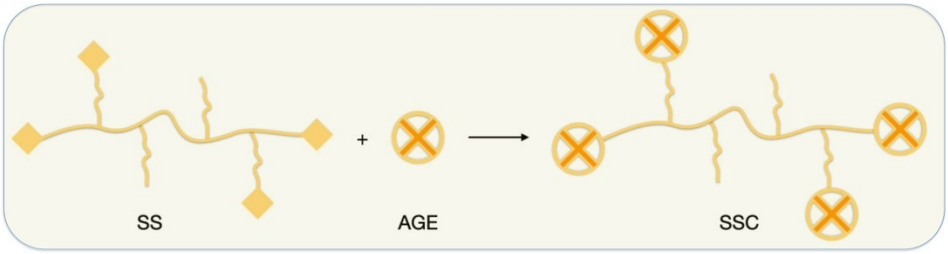

c

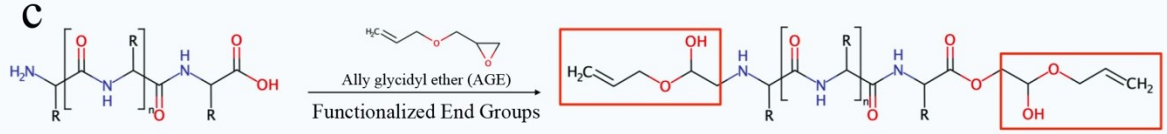

Silk Sericin (SS)
(Representative structure)

Silk Sericin Multifunctional
Crosslinker (SSC)

d

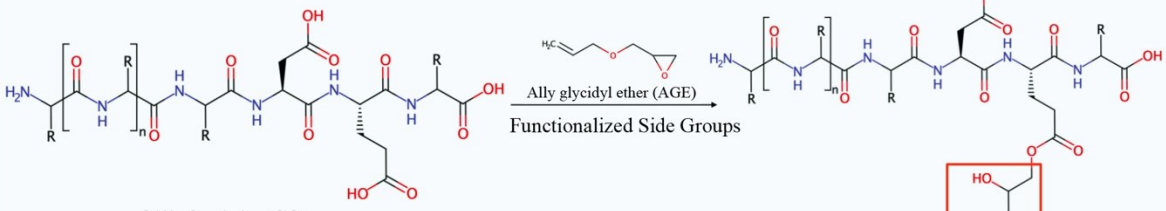

Silk Sericin (SS)
(Showing aspartic and glutamic acid
amino acid reaction)

Silk Sericin Multifunctional
Crosslinker (SSC)

Figure 2. Silk sericin multifunctional crosslinker (SSC) synthesis: (a) The most common amino acids found in silk sericin (31–33); (b), (c) and (d) show the chemical functionalization, showing a cartoon schematic (b), end group functionalization (c) and side group functionalization (d).

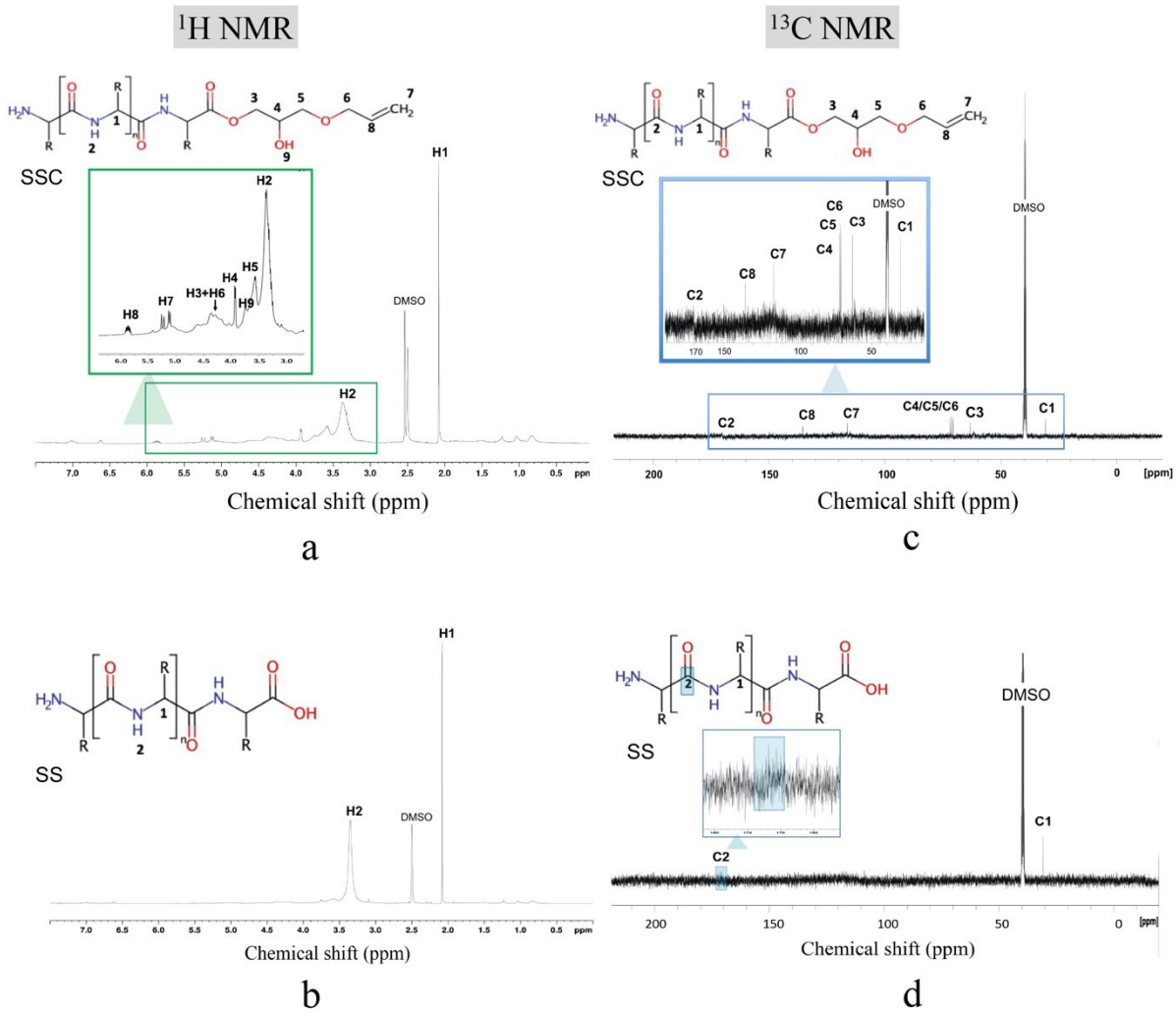

Figure 3. Silk sericin multifunctional crosslinker (SSC) synthesis: (a) ^{1}H NMR spectrum of SSC; (b) ^{1}H NMR spectrum of SS; (c) ^{13}C NMR spectrum of SSC and (d) ^{13}C NMR spectrum of SS.

The ^{1}H NMR spectrum of SSC (Fig.3a) shows proton peaks from the modification at H3 and H6, H4, H9 (hydroxyl group), H5, H7 and H8 (vinyl group) at 4.2, 3.8, 3.7, 3.5, 5.2 and 5.9 ppm, respectively. From the ^{13}C NMR spectrum of SSC (Fig.3c), the modified carbons (C3, C4, C7 and C8) show peaks at 63.1, 70.6, 116.1 and 135.4 ppm, respectively. Both were compared with the ^{1}H NMR spectrum of SS (Fig.3b) and ^{13}C NMR spectrum of SS (Fig.3d), respectively. In short, the results from both ^{1}H and ^{13}C NMR spectroscopies confirm the successful incorporation of vinyl groups to SS. FTIR spectroscopy was also used to provide further evidence of the modification step. The FTIR spectrum of SSC was compared with the spectrum of SS, as shown in Fig.4. The peak of C-H bending vinyl groups (953-932 cm^{-1}) of AGE in SSC are observed. Also, there is a shift in the FTIR spectrum of

SSC to a lower wavenumber when compared to SS. This might be because the AGE addition results in a change to the stiffness of the SS chains. In addition, the N-H stretching band in SSC appears at lower frequency and sharper than that in SS, due to a reduction in the degree of hydrogen bonding, following the conversion of several carboxylic acid groups and an amine group.

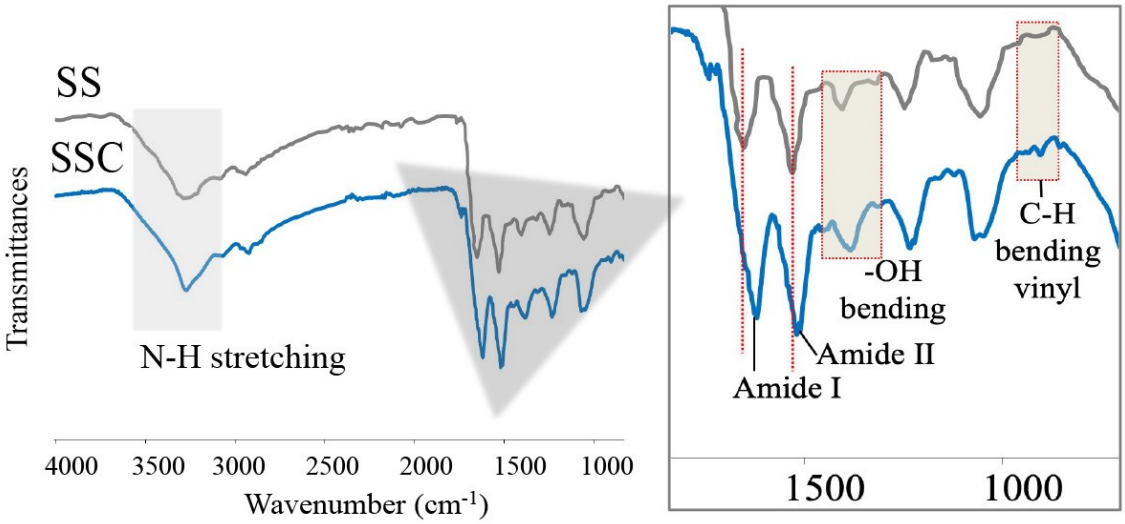

Figure 4. FTIR spectrum of silk sericin (SS) and silk sericin multifunctional crosslinker (SSC).

Poly(lactic acid) macromonomer (PLAM)

PLAM was modified through the reaction of allyl glycidyl ether (AGE) in the presence of zinc and low molecular weight PLA (M_w ~ 2,250 g/mol), which follows the same reaction pathway to SSC by opening the epoxide ring of AGE at the chain-ends of PLA (as shown in Fig.5a). The chemical structure and functional groups of PLAM were analyzed. From ^{1}H NMR spectrum of PLAM (Fig.5b), the proton peaks at H3 and H6, H4, H9 (hydroxyl group), H5 from the opened epoxide ring of AGE were observed at 4.2, 4.0, 3.6 and 3.5 ppm, respectively. While the proton peaks at H7 and H8 of the vinyl group were observed at 5.2 and 5. 5 ppm. The ^{13}C NMR spectrum of PLAM (Fig.5d) was also analyzed. The carbon peaks at C1, C2, C3, C4, C5, C6 and C7 were observed at 16.1, 68.6, 169.1, 65.7, 66.0, 70.5 and at approximately 68.5 ppm. Both were also compared with ^{1}H NMR spectrum of PLA (Fig.5c) and ^{13}C NMR spectrum of PLA (Fig.5e), respectively. Thus, the carbon

peaks at C4-C9, plus the results from ^{1}H NMR confirm the presence of AGE at the chain-ends of PLAM and the successful modification of PLA.

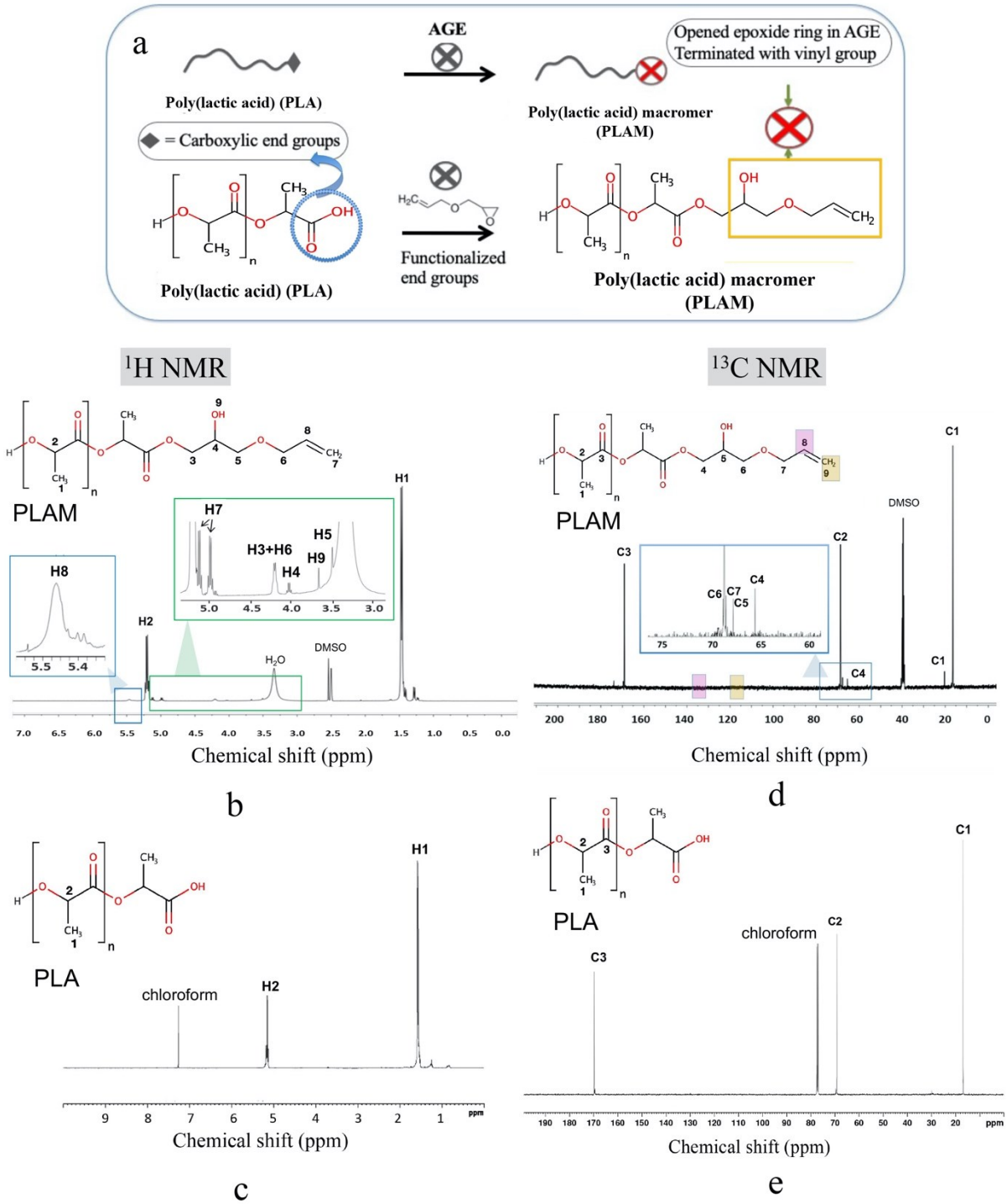

Figure 5. Poly(lactic acid) macromonomer (PLAM): (a) reaction of functionalized poly(lactic acid) (PLA); (b) ^{1}H NMR spectrum of PLAM; (c) ^{1}H NMR spectrum of PLA; (d) ^{13}C NMR spectrum of PLAM; and (e) ^{13}C NMR spectrum of PLA.

FTIR was also used to confirm the successful modification of the chain-ends of PLAM (see Fig.6). FTIR spectrum of PLAM was compared with the spectrum of PLA. The C-H stretching band at 2960-3150 cm^{-1} from both PLA and PLAM was observed. However, vinyl C-H bending at 952 cm^{-1} and O-H bending (out-of-plane) at 900 cm^{-1} were only observed in PLAM (inset). In addition, the bands at 1665 cm^{-1} and 1415 cm^{-1} in PLAM, are attributed to C=C stretching and C-O-H bending (in-plane), respectively. In contrast, these bands are not observed in unmodified PLA. The PLAM spectrum also shows a band from -OH bending, which originates from the opened epoxide ring.

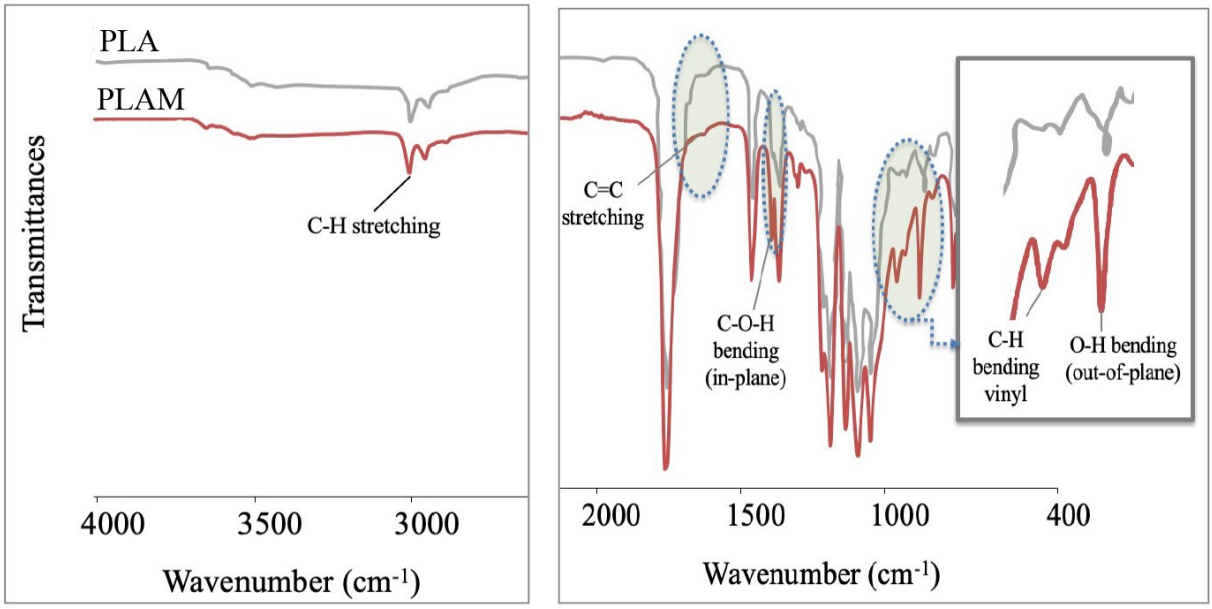

Figure 6. FTIR spectra of poly(lactic acid) (PLA) and poly(lactic acid) macromonomer (PLAM).

3.2 Nanogels of PLAM/SSC: Effect of *N*′,*N*-mBAAm crosslinker

Modified SSC and PLAM were used to fabricate nanogels via conventional free radical polymerization. An additional short-chain bifunctional chemical crosslinker (0.5% *N*′,*N*-mBAAm) was employed to allow a degree of control over the properties of the final nanogels. These chemically crosslinked nanogels are referred to as *crosslinked-PLAM*, *crosslinked-SSC*, and *crosslinked PLAM/SSC* throughout this manuscript. The effect of different *N*′,*N*-mBAAm contents was studied in terms of morphology, *in vitro* drug release profiles and *in vitro* cytotoxicity.

Morphology

The morphology of crosslinked-PLAM, crosslinked-SSC and crosslinked PLAM/SSC (with 0, 0.5, 1.0, 1.5 and 2% w/w *N*′,*N*-mBAAm) were analyzed by TEM, as shown in Fig.7A, together with schematic illustrations of the comparision of diameter sizes of crosslinked-PLAM/SSC nanogels with different concentrations of *N*′,*N*-mBAAm. The crosslinked-PLAM and crosslinked-SSC show particles of irregular spherical shape, which have diameters in the range of 30-50 nm and 60-80 nm, respectively. The crosslinked-PLAM particles are smaller and more irregular than those of SSC. This is possibly due to the fact that PLAM contains a smaller number of vinyl ended-chains and also has the potential to chain extend, forming longer chains of PLA instead of forming a crosslinked structure. Whereas SSC possesses more carboxylic groups both at the chain-ends and also as pendant side-groups, which are able to subsequently generate higher numbers of crosslinked structures.

Comparing crosslinked-PLAM/SSC nanogels with 0% and 0.5% *N*′,*N*-mBAAm, the nanogels containing additional *N*′,*N*-mBAAm crosslinker have better homogeneity with uniform spherical shape and are approximately five times larger in diameter than the crosslinked-PLAM/SSC nanogels without *N*′,*N*-mBAAm. This is attriubted to the hydrophilic nature of the crosslinker (*N*′,*N*-mBAAm) – solubility in water: 19.4 mM (34), so when the nanogel starts is being formed the nuclei can imbibe an considerable amount of any aqueous monomer solution (35). In our system, the solvent for SSC is water, therefore this results in a larger size of *N*′,*N*-mBAAm – containing crosslinked-PLAM/SSC nanogels.

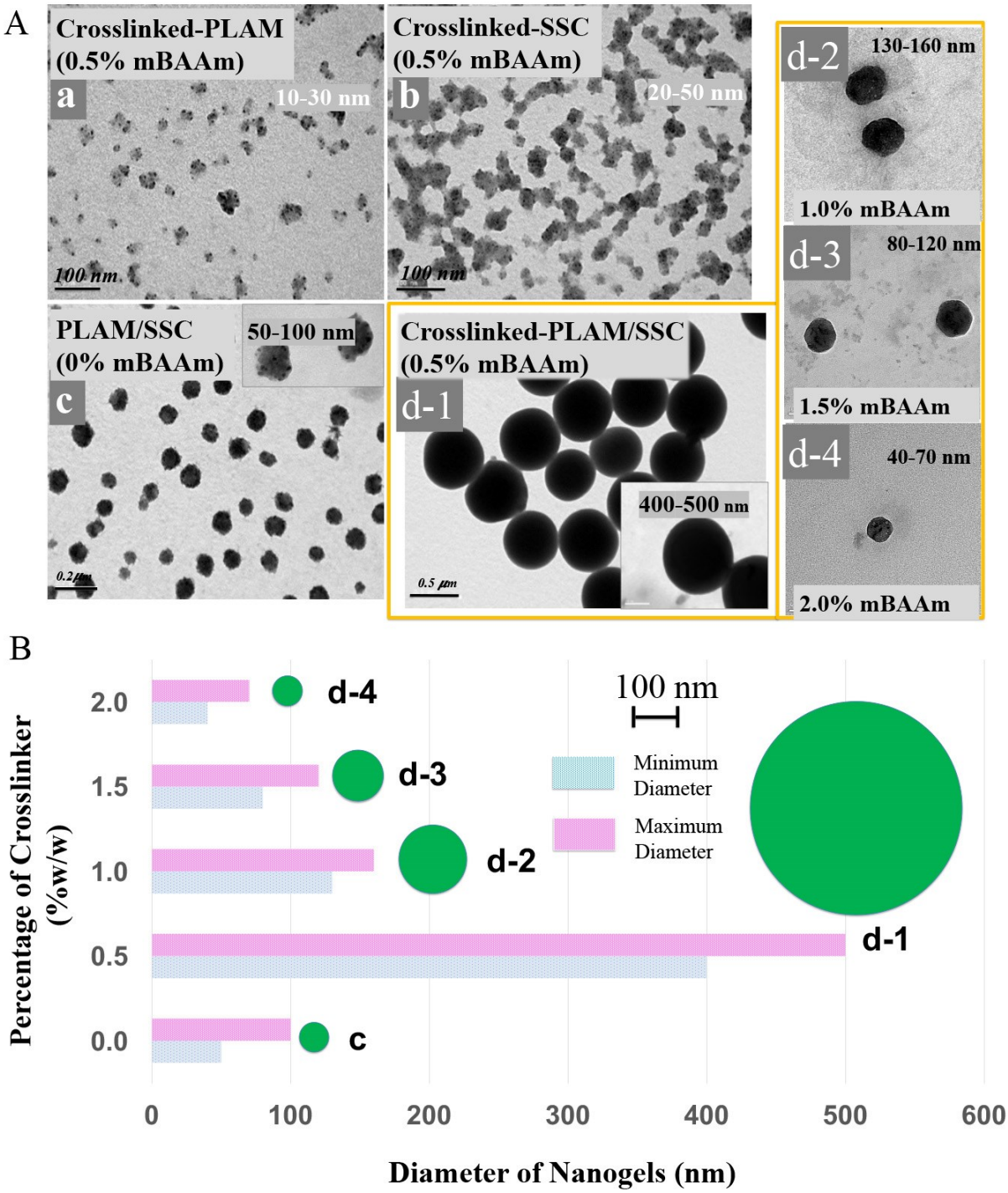

Figure 7. (A) TEM images of crosslinked-PLAM, crosslinked-SSC and crosslinked-PLAM/SSC at 0, 0.5, 1.0, 1.5 and 2.0% w/w *N*′,*N*-mBAAm, prepared by suspension in PBS (pH 7.4) prior to dropping onto a carbon grid; (B) Diameters of crosslinked-PLAM/SSC at different concentrations of *N*′,*N*-mBAAm.

In this work, we also studied the effect of *N*′,*N*-mBAAm crosslinker concentration (0, 0.5, 1.0, 1.5 and 2.0 % w/w) on the diameter of the nanogel particles, as the size of the nanogels will influence their performance in any desired application (36). The results are shown in Fig.7B and show that as higher concentrations of *N*′,*N*-mBAAm crosslinker were used (>1.0%), smaller particles were observed. This is similar to conventional hydrogels in that as the amount of crosslinker increases, there is a decrease in the ability for the gels to swell because the crosslinks create more constraints preventing swelling. When no additional crosslinker is presented (0% *N*′,*N*-mBAAm), only the multifunctional SSC can react to form the nanogel particles. However, this results in particles having small diameters and not being homogeneous or smooth spheres.

In vitro drug release and in vitro cytotoxicity

The *in vitro* drug release profiles of crosslinked-PLAM/SSC nanogels at 0, 0.5, 1.0, 1.5 and 2.0 %w/w *N*′,*N*-mBAAm crosslinker were tested for 48 hrs, as shown in Fig.8a. It is important to note that all nanogels were saturated with a constant concentration of model drug. The data show that crosslinked PLAM/SSC nanogels at 0.5%w/w *N*′,*N*-mBAAm released rhodamine B (a hydrophilic dye as model drug) with a cumulative release of over 80%. A rapid release was observed during the first 4 hours, followed by a gradual reduction in release between 4 and 8 hours before tailing off towards the end of the testing period (48 hours). Samples with higher levels of crosslinking showed the same trend in release profiles, albeit their cumulative release was much lower than that of crosslinked-PLAM/SSC at 0.5%XL. The nanogels at 1.0, 1.5 and 2.0 %w/w *N*′,*N*-mBAAm had cumulative release percentages of 47%, 40% and 30%, respectively. The release profiles show that higher crosslinker concentrations gave lower cumulative release, due to smaller particle size of the nanogels resulting in a reduction of drug load within the particles. In addition, higher crosslink density and greater molecular interactions between PLA, SS, hydrophilic crosslinker and the hydrophilic model drug may effect to the release of the model drug. Therefore, the crosslinked-PLAM/SSC nanogels at 0.5 %XL-PLAM/SSC nanogels were chosen to study further due to demonstrating good spherical shape, homogeneity and good uptake and release of hydrophilic model drug.

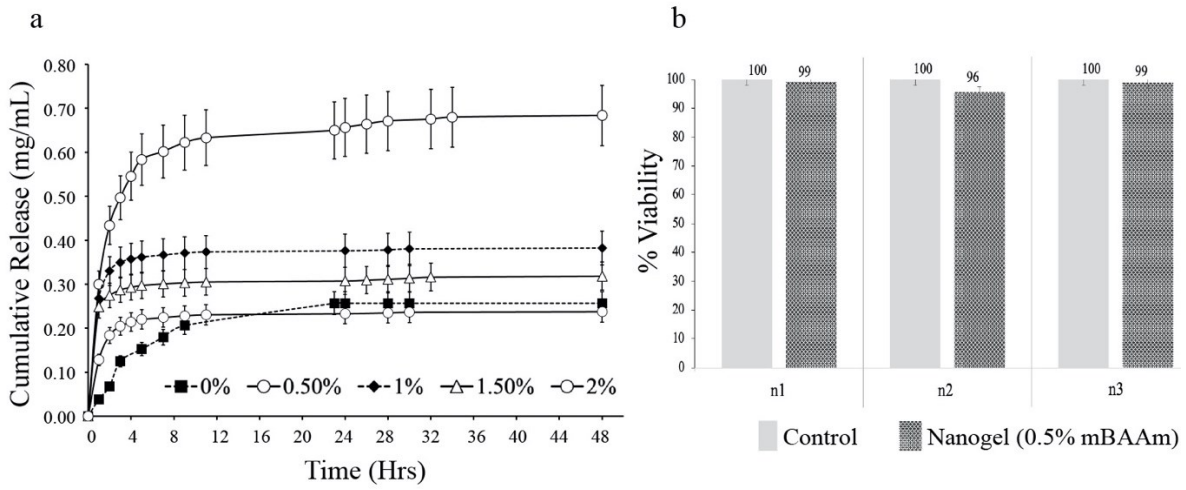

Figure 8. (a) *In vitro* drug release profile of crosslinked-PLAM/SSC at different concentrations of *N*′,*N*-mBAAm; (b) *in vitro* cytotoxicity of crosslinked-PLAM/SSC at 0.5%w/w of *N*′,*N*-mBAAm (n = 3), the DMEM culture medium without nanogels was used as a control (p values >0.05 for all samples).

In vitro cytotoxicity of crosslinked-PLAM/SSC nanogels at 0.5%XL were measured using an XTT assay. Figure 8b shows cell cytotoxicity by measuring % cell viability via the OD value at 490 nm, using NHSF cell line for 24 hrs. The DMEM culture medium without nanogels was used as a control. The results show that the % cell viability of triplicate tests of nanogels were over 90% of control. There is no significant difference in cell viability of all the control and nanogels. The cell viability study suggests that this crosslinked-PLAM/SSC nanogels is non-toxic to the NHSF cells line.

In summary, crosslinked-PLAM/SSC nanogels were successfully fabricated through the synthesis of a PLA macromonomer and SS multifunctional crosslinker, showing good release kinetics of hydrophilic model drug and were non-toxic to NHSF cell lines. Therefore, these novel bio-derived nanogels have potential for use as antibiotic drug (typically hydrophilic) carriers in the field of tissue repair and regeneration. As a demonstration of the potential of our nanogels, we investigated their utility as embedded nanoparticles in electrospun fibers for future use in tissue engineering.

3.3 Incorporation of nanogels into PLGA electrospun fiber meshes

As aforementioned, tissue engineering scaffolds in the form of electrospun nanofibers have been of interest for use in tissue repair due to their morphological similarity to the extracellular matrix (ECM) (37–41). Electrospun nanofibers have many unique properties, as

electrospinning produces ultrafine fibers with small diameters, which leads to high surface area-to-volume ratios, high porosities with small pores, high liquid absorption capacity and water vapor permeability. These properties allow nano- and microfibers to have excellent interactions with skin or damaged tissue (42). Thus, our crosslinked-PLAM/SSC (at 0.5%XL) nanogels were embedded into electrospun nanofibrous fabrics of PLGA (a biodegradable and compatible polymer) to create a multifunctional, composite scaffold from fully biodegradable materials. The role of the nanogel particles is to increase the hydrophilicity of PLGA nanofibers for enhanced contact with skin or wounds. The hybrid scaffold should also improve the efficiency of release of hydrophilic bioactive agents that are added and held in the crosslinked-PLAM/SSC nanogels, which are embedded in the PLGA nanofibers.

Morphology, in vitro degradation and hydrophilicity

Figure 9a shows SEM images of the PLGA nanofibrous fabrics. The morphology comprises continuous smooth homogeneous fibers with random orientation and diameters in the range of 700-1000 nm. Incorporation of PLAM/SSC nanogel particles into the PLGA nanofibrous mesh was confirmed by the presence of spherical entities in the SEM images (Fig.9b) and TEM image (Fig.9e). Interestingly, the incorporation of nanogel particles did not affect the smooth morphology of the fibers or effect the average fibers diameter sizes.

The rationale in fabricating this scaffold was for skin tissue regeneration, therefore, the degradation and hydrophilicity of the polymer matrices are important properties. Generally, PLGA tends to degrade via bulk erosion without a constant erosion velocity (43). Therefore, changes in morphology (observed by SEM) after submerging the scaffold in DI-water for 2 weeks was preliminarily used to observe the degradation of our hybrid meshes (Fig.9c and 9d). After soaking, the PLGA electrospun nanofibers swell and lose their uniform shape, while some of the crosslinked-PLAM/SSC nanogels are observed at the fiber surface instead of embedded within the fibers. This phenomenon helps to support that the release of drugs from the embedded nanogels can occur without complete surface erosion.

The percentage of accumulative enzymatic degradation of the electrospun nanofibers embedded with nanogels was observed from weeks 1 to 11 (Fig.10). Degradation of the hybrid fabrics increased continuously over time and reached ~80% at week 11, while that of PLGA nanofibers without nanogel particles only reached ~50%. The degradation of PLGA is generally known that it occurs through hydrolysis, which causes chain cleavage and the

PLGA matrix changes and undergoes bulk erosion (43). Therefore the nanofibers containing nanogels are more hydrophilic and thus increase the degradation rate.

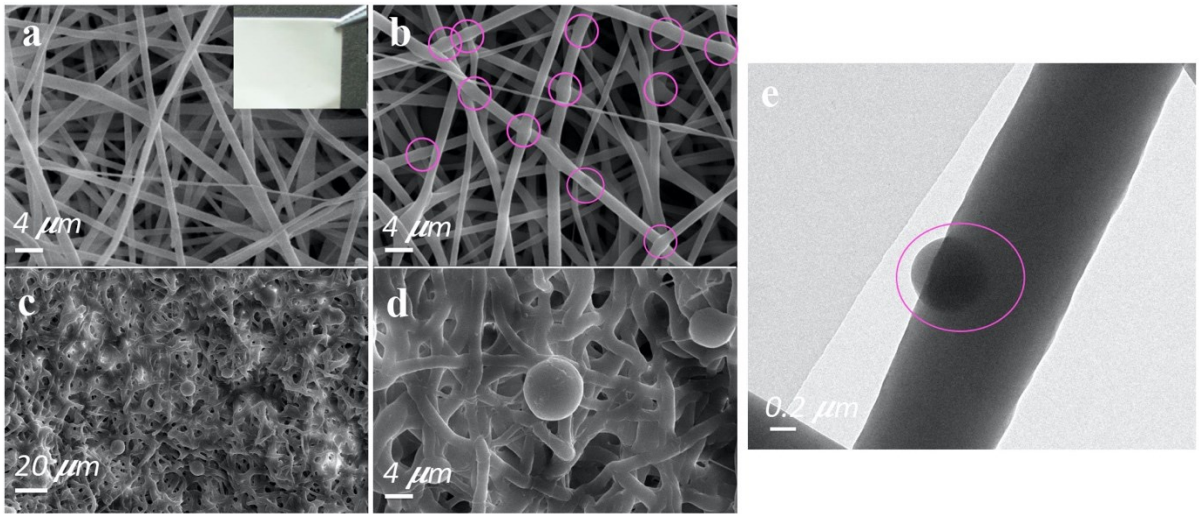

Figure 9. SEM images of (a) PLGA nanofiber (inset - fiber fabric), (b) PLGA/nanogel nanofiber, (c,d) PLGA/nanogel nanofiber submersed in DI water for 2 weeks at magnification of 500x and 2000x, respectively, and (e) TEM images of PLGA nanofiber cooperated with nanogel.

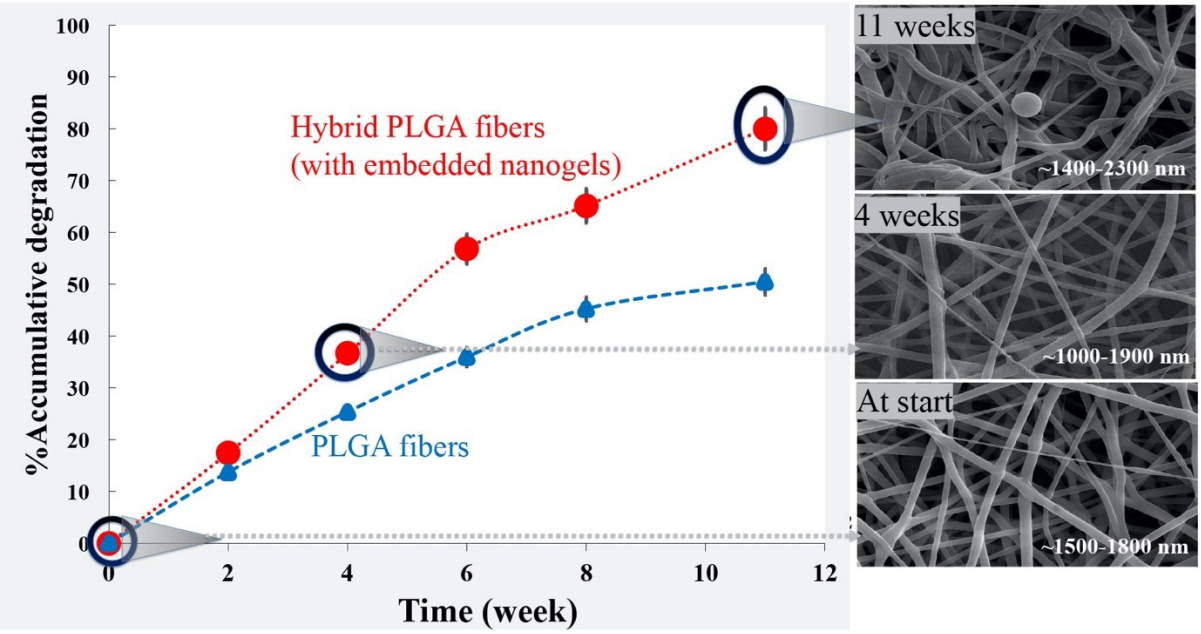

Figure 10. Percentage of enzymatic accumulative degradation of hybrid PLGA nanofibers (with embedded nanogels) at different times performed at 37ºC in 0.004 % trypsin in PBS solution (pH 7.4), together with SEM images (magnification of 2K) at the start, and after 4 and 11 weeks of degradation.

The hydrophilicity of PLGA nanofibers and embedded nanogel-PLGA nanofibers were observed using static contact angle measurements over a time period of 10 minutes (Fig.11). Both systems show similar hydrophilicity when the water droplet is first deposited. However, as contact time increased, the nanofibers with embedded nanogel particles become increasingly more hydrophilic than the PLGA nanofibers over the entire testing time period, with the difference (1° at the start to 20° after 10 minutes) increasing as time increased. These results show that the idea of incorporation of crosslinked-PLAM/SSC nanogels into the PLGA nanofibers for the enhancement of skin and wound contact was successful and will be beneficial for further use in tissue engineering.

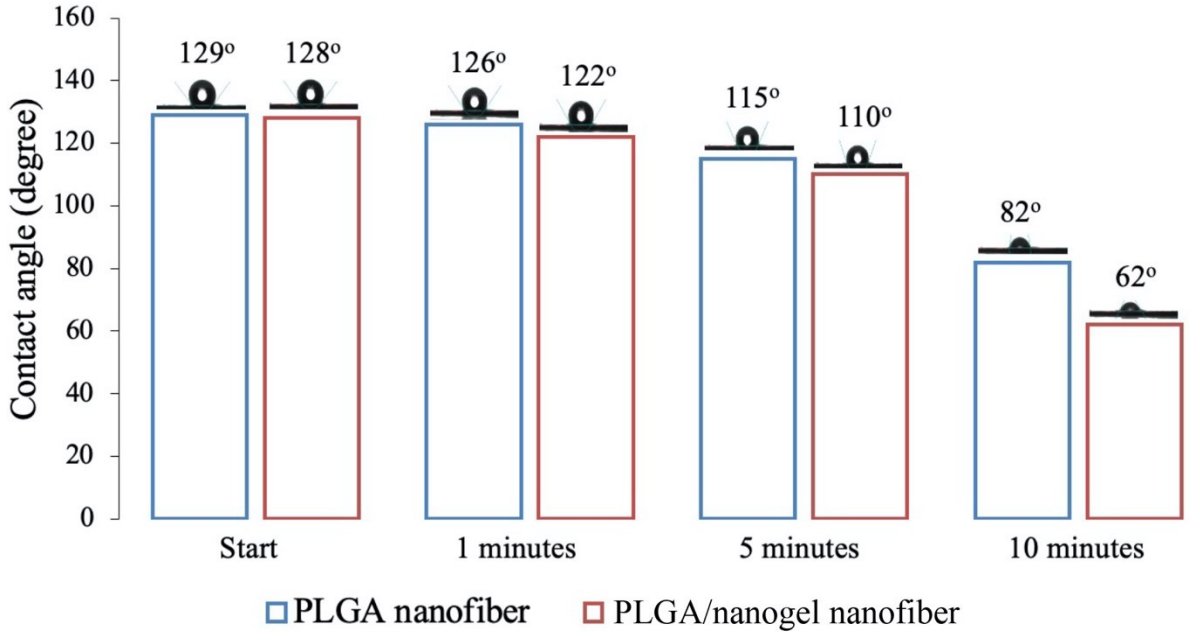

Figure 11. Water contact angles of PLGA electrospun nanofibers and PLGA electrospun nanofibers embedded crosslinked-PLAM/SSC nanogels.

Cell proliferation

The *in vitro* cell proliferation of PLGA nanofibers, PLGA embedded crosslinked-PLAM/SSC nanogels and PLGA/nanogel/RhB nanofibers were studied using a XTT assay (Fig.12a). Results show that all samples were non-toxic to normal human skin fibroblast cell line (NHSF) and metabolically active cells reduce the yellow tetrazolium salt or XTT to an orange formazan dye. If there is an enhancement in the number of living cells, this results in

higher activity of mitochondrial dehydrogenases in the samples and thus a higher OD was observed. The results show that the NHSF cell lines grew or proliferate in all PLGA/nanogel nanofibers and PLGA/nanogel/RhB nanofibers after 1 day of culture similar to the PLGA nanofibers. The increase in cell proliferation is observed in all samples at days 3 and 5 of culture. In addition, PLGA fibers embedded with crosslinked-PLAM/SSC nanogels show better cell growth at days 3 and 5 when compared to that of PLGA fibers alone. The optical images also showed the morphology of living NHSF cell line from well plate with and without PLGA/nanogel nanofibers (Fig.12b). This shows that these electrospun nanofibers embedded nanogels can be used as biocompatible materials for medical devices.

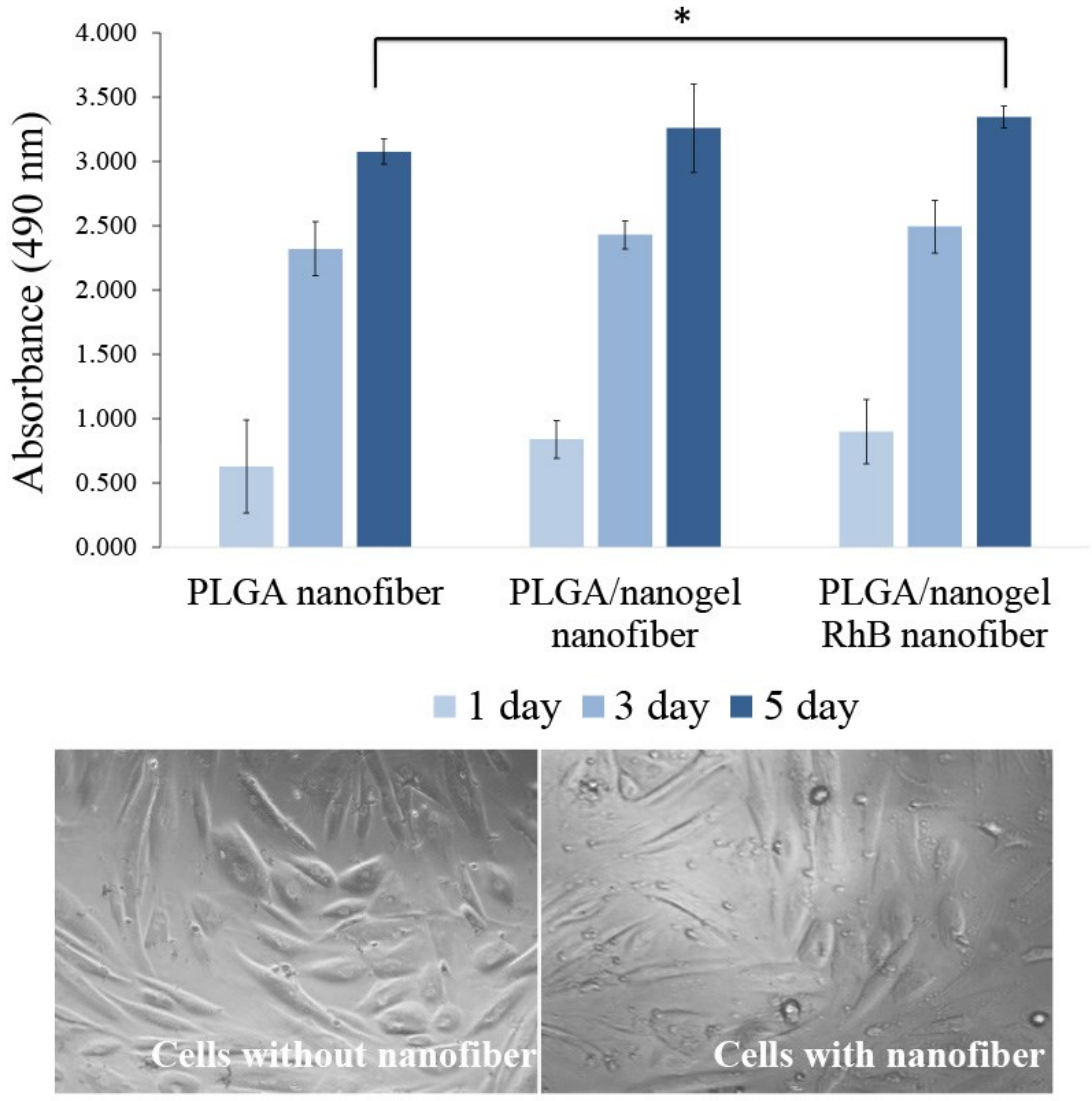

Figure 12. (a) *In vitro* cell proliferation of PLGA nanofiber, PLGA/nanogel nanofiber and PLGA/nanogel/RhB nanofibers at day 1, 3 and 5 (* p value <0.05) (b) the optical images of NHSF cell lines from well plate with and without nanofibers.

4. Conclusions

Novel nanogels based on low molecular weight of PLA and SS, a synthetic and natural biodegradable and biocompatible materials, were synthesized for the first time. Low molecular weight PLA and SS were successfully modified to alter their carboxyl and amine chain-ends or side groups to be the polymerizable PLA and SS, termed “PLAM and SSC”. The nanogels of crosslinked PLAM/SSC show different diameter size and drug release profiles depending on the concentration of crosslinker in which higher crosslinker concentrations resulted in smaller diameter sizes and lower drug release. The nanogels were non-toxic to NHSF cell lines. PLAM/SSC nanogels with 0.5% w/w crosslinker with a diameter size of 400-500 nm were embedded within PLGA electrospun nanofibers. The nanogels enhance the hydrophilicity of the PLGA electrospun nanofibers. The electrospun nanofibers embedded nanogels were non-toxic to the NHSF cell lines and enzymatic degradable with good cell proliferation. With the inherent advantages and good properties of the fabricated nanogels of PLAM/SSC and embedded nanogel-PLGA nanofibers, these materials have the potential for use not only in a field of drug delivery but also in tissue regeneration.

Acknowledgements

This work was funded by Thailand Science Research and Innovation (TSRI) (Grant Number R2565B062) and has received funding from the European Union’s Horizon 2020 research and innovation programme under the Marie Sklodowska-Curie grant agreement No 871650. This research was also partially supported by the Program Management Unit for Human Resources & Institutional Development, Research and Innovation, Office of National Higher Education Science Research and Innovation Policy Council (NXPO), Thailand [Grant Number B16F640001] and Center of Excellence in Materials Science and Technology, Chiang Mai University. Also, thanks to the Science Lab Centre, Faculty of Science, Naresuan University for supporting XRD, DSC, CA, SEM and FTIR measurements.

Data Availability

The raw/processed data required to reproduce these findings cannot be shared at this time as the data also forms part of an ongoing study.

References

1. Anooj ES, Charumathy M, Sharma V, Vibala B V, Gopukumar ST, Jainab SIB, et al. Nanogels: An overview of properties, biomedical applications, future research trends and developments. J Mol Struct. 2021;1239:130446
2. Ahmed S, Alhareth K, Mignet N. Advancement in nanogel formulations provides controlled drug release. Int J Pharm. 2020;584:119435
3. Oh JK, Drumright R, Siegwart DJ, Matyjaszewski K. The development of microgels/nanogels for drug delivery applications. Prog Polym Sci. 2008;33(4):448–77.
4. McClements DJ. Designing biopolymer microgels to encapsulate, protect and deliver bioactive components: Physicochemical aspects. Adv Colloid Interface Sci. 2017;240:31–59.
5. Feng Q, Li D, Li Q, Cao X, Dong H. Microgel assembly: Fabrication, characteristics and application in tissue engineering and regenerative medicine. Bioact Mater. 2022;9:105-119.
6. Xiong MH, Bao Y, Yang XZ, Zhu YH, Wang J. Delivery of antibiotics with polymeric particles. Adv Drug Deliv Rev. 2014;78:63–76.
7. Keskin D, Zu G, Forson AM, Tromp L, Sjollema J, van Rijn P. Nanogels: A novel approach in antimicrobial delivery systems and antimicrobial coatings. Bioact Mater. 2021;6:3634-57.
8. Lecaroz MC, Blanco-Prieto MJ, Campanero MA, Salman H, Gamazo C. Poly(D,L-lactide-coglycolide) particles containing gentamicin: Pharmacokinetics and pharmacodynamics in Brucella melitensis-infected mice. Antimicrob Agents Chemother. 2007;51(4):1185–90.
9. Ungaro F, D'Angelo I, Coletta C, D'Emmanuele Di Villa Bianca R, Sorrentino R, Perfetto B, et al. Dry powders based on PLGA nanoparticles for pulmonary delivery of antibiotics: Modulation of encapsulation efficiency, release rate and lung deposition pattern by hydrophilic polymers. J Control Release. 2012;157(1):149-59.
10. Calvo P, Sánchez A, Martínez J, López MI, Calonge M, Pastor JC, et al. Polyester nanocapsules as new topical ocular delivery systems for cyclosporin A. Pharm Res. 1996;13(2):311-15.
11. Rassu G, Gavini E, Jonassen H, Zambito Y, Fogli S, Breschi MC, et al. New chitosan derivatives for the preparation of rokitamycin loaded microspheres designed for ocular or nasal administration. J Pharm Sci. 2009;98(12): 4852-65.
12. Ross S, Mahasaranon S, Ross GM. Ternary polymer blends based on poly(lactic acid):

Effect of stereo-regularity and molecular weight. J Appl Polym Sci. 2015;132(14):41780(1-8).
13. Ross S, Topham PD, Tighe BJ. Identification of optically clear regions of ternary polymer blends using a novel rapid screening method. Polym Int. 2014;63(1):44–51.
14. Yooyod M, Ross GM, Limpeanchob N, Suphrom N, Mahasaranon S, Ross S. Investigation of silk sericin conformational structure for fabrication into porous scaffolds with poly(vinyl alcohol) for skin tissue reconstruction. Eur Polym J. 2016;81:43–52.
15. Zhang YQ. Applications of natural silk protein sericin in biomaterials. Biotechnol Adv. 2002;20(2): 91-100.
16. Lamboni L, Gauthier M, Yang G, Wang Q. Silk sericin: A versatile material for tissue engineering and drug delivery. Biotechnol Adv. 2015;33(8):1855–67.
17. Ho MP, Wang H, Lau KT, Lee JH, Hui D. Interfacial bonding and degumming effects on silk fibre/polymer biocomposites. Compos Part B Eng. 2012;43(7): 2801-12.
18. Aramwit P, Siritientong T, Srichana T. Potential applications of silk sericin, a natural protein from textile industry by-products. Waste Manag Res. 2012; 30(3):217-24.
19. O'Brien FJ. Biomaterials & scaffolds for tissue engineering. Mater Today. 2011;14(3):88–95.
20. Zhong SP, Zhang YZ, Lim CT. Tissue scaffolds for skin wound healing and dermal reconstruction. Wiley Interdiscip Rev Nanomed Nanobiotechnol. 2010;2(5):510–25.
21. Ross S, Yooyod M, Limpeanchob N, Mahasaranon S, Suphrom N, Ross GM. Novel 3D porous semi-IPN hydrogel scaffolds of silk sericin and poly(N-hydroxyethyl acrylamide) for dermal reconstruction. Express Polym Lett. 2017;11(9): 719-30.
22. Zhou XH, Wei DX, Ye HM, Zhang X, Meng X, Zhou Q. Development of poly(vinyl alcohol) porous scaffold with high strength and well ciprofloxacin release efficiency. Mater Sci Eng C. 2016;67:326–35.
23. Mehrasa M, Asadollahi MA, Ghaedi K, Salehi H, Arpanaei A. Electrospun aligned PLGA and PLGA/gelatin nanofibers embedded with silica nanoparticles for tissue engineering. Int J Biol Macromol. 2015;79:687–95.
24. Dias JR, Baptista-Silva S, Sousa A, Oliveira AL, Bártolo PJ, Granja PL. Biomechanical performance of hybrid electrospun structures for skin regeneration. Mater Sci Eng C. 2018;93(August):816–27.
25. Kumkun P, Tuancharoensri N, Ross G, Mahasaranon S, Jongjitwimol J, Topham PD, et al. Green fabrication route of robust, biodegradable silk sericin and poly(vinyl

alcohol) nanofibrous scaffolds. Polym Int. 2019;68(11):1903-13.
26. Tuancharoensri N, Ross GM, Mahasaranon S, Topham PD, Ross S. Ternary blend nanofibres of poly(lactic acid), polycaprolactone and cellulose acetate butyrate for skin tissue scaffolds: influence of blend ratio and polycaprolactone molecular mass on miscibility, morphology, crystallinity and thermal properties. Polym Int. 2017;66(11):1463-72.
27. Agarwal S, Wendorff JH, Greiner A. Use of electrospinning technique for biomedical applications. Polymer. 2008;49:5603-21.
28. Liu X, Nielsen LH, Kłodzińska SN, Nielsen HM, Qu H, Christensen LP, et al. Ciprofloxacin-loaded sodium alginate/poly (lactic-co-glycolic acid) electrospun fibrous mats for wound healing. Eur J Pharm Biopharm. 2018;123(November 2017):42–9.
29. Zhang L, Wang Z, Xiao Y, Liu P, Wang S, Zhao Y, et al. Electrospun PEGylated PLGA nanofibers for drug encapsulation and release. Mater Sci Eng C. 2018;91(May):255–62.
30. Lalit Jajpura AR. The Biopolymer Sericin: Extraction and Applications. J Text Sci Eng. 2015;05:188.
31. Kunz RI, Brancalhão RMC, Ribeiro LDFC, Natali MRM. Silkworm Sericin: Properties and Biomedical Applications. Biomed Res Int. 2016;2016:8175701.
32. Mondal M, Trivedy K. The silk proteins, sericin and fibroin in silkworm, Bombyx mori Linn., - a review. Casp J Env Sci. 2007;5(2):63–76.
33. Rajput SK, Kumar Singh M. Sericin – A unique biomaterial. IOSR J Polym Text Eng 2015;2(3):2348–181.
34. Imaz A, Forcada J. N-vinylcaprolactam-based microgels: Effect of the concentration and type of cross-linker. J Polym Sci Part A Polym Chem. 2008;46(8):2766-75.
35. Obeso-Vera C, Cornejo-Bravo JM, Serrano-Medina A, Licea-Claverie A. Effect of crosslinkers on size and temperature sensitivity of poly(N-isopropylacrylamide) microgels. Polym Bull. 2013;70(2):653-64.
36. Chu Y, Jo Y, Chen L. Size-controllable core/shell whey protein microgels with narrow particle size distribution fabricated by a facile method. Food Hydrocoll. 2021;124(PB):107316.
37. Sill TJ, von Recum HA. Electrospinning: Applications in drug delivery and tissue engineering. Biomaterials. 2008;29:1989-2006.
38. Pham QP, Sharma U, Mikos AG. Electrospinning of polymeric nanofibers for tissue

engineering applications: A review. Tissue Eng. 2006;12(5):1197-211.
39. Rahmati M, Mills DK, Urbanska AM, Saeb MR, Venugopal JR, Ramakrishna S, et al. Electrospinning for tissue engineering applications. Prog Mater Sci. 2021;117:100721.
40. Liu H, Ding X, Zhou G, Li P, Wei X, Fan Y. Electrospinning of nanofibers for tissue engineering applications. J Nanomater. 2013;2013:1-11.
41. Tuancharoensri N, Ross G, Punyodom W, Mahasaranon S, Jongjitwimol J, Topham PD, et al. Multifunctional core-shell electrospun nanofibrous fabrics of poly(vinyl alcohol)/silk sericin (core) and poly(lactide- co -glycolide) (shell). Polym Int. 2021;71(3):266-75.
42. Dwivedi C, Pandey I, Pandey H, Ramteke PW, Pandey AC, Mishra SB, et al. Chapter 9-Electrospun Nanofibrous Scaffold as a Potential Carrier of Antimicrobial Therapeutics for Diabetic Wound Healing and Tissue Regeneration. Nano- and Microscale Drug Delivery Systems: Design and Fabrication. Elsevier Inc. 2017:147–164.
43. Burkersroda F Von, Schedl L, Göpferich A. Why degradable polymers undergo surface erosion or bulk erosion. Biomaterials. 2002;23(21):4221-31.